ICASE

ON CONFORMING MIXED FINITE ELEMENT METHODS FOR

INCOMPRESSIBLE VISCOUS FLOW PROBLEMS

Max D. Gunzburger

R. A. Nicolaides

and

Janet S. Peterson

Report No. 81-23

July 31, 1981

INSTITUTE FOR COMPUTER APPLICATIONS IN SCIENCE AND ENGINEERING

NASA Langley Research Center, Hampton, Virginia 23665

Operated by the

UNIVERSITIES SPACE USRA RESEARCH ASSOCIATION

ON CONFORMING MIXED FINITE ELEMENT METHODS FOR INCOMPRESSIBLE VISCOUS FLOW PROBLEMS

Max D. Gunzburger
University of Tennessee, Knoxville

R. A. Nicolaides
Carnegie-Mellon University

and

Janet S. Peterson
University of Pittsburgh

ABSTRACT

The asymptotic rates of convergence for approximate solutions of linearizations of the stationary Navier-Stokes equations are computationally determined for some specific choices of conforming finite element spaces. These rates are computed for norms of physical interest and are compared to available theoretical estimates. It is shown that equivalent rates of convergence are achieved by alogrithms which differ greatly in their computer storage and time requirements. The solution of the discrete system of equations resulting from the finite element discretization is also discussed.

This research was supported by the Air Force Office of Scientific Research under Grant Nos. AF-AFOSR-80-0083 and AF-AFOSR-80-0091. Partial support was also provided by NASA Contract No. NAS1-15810 while the authors were in residence at the Institute for Computer Applications in Science and Engineer, NASA Langley Research Center, Hampton, VA 23665.

1. Introduction

We consider the approximate solution of linearizations of the Navier-Stokes equations of viscous incompressible flow. In particular we are concerned with conforming mixed finite element methods. We make no attempt here to solve the full nonlinear Navier-Stokes equations, but certainly the results and algorithms discussed below have considerable relevance to that case. For instance, many iterative algorithms for the approximate solution of the nonlinear Navier-Stokes equations require, for each iteration, the approximate solution of a linear problem of the type we consider here.

Our first goal is to examine the rates of convergence of some particular finite element approximations. These rates will be determined for norms of physical interest. These are the L^2-norms for the pressure and the $\vec{L}^2$ and $\vec{H}^1$-norms for the velocity field. The latter are of interest in the calculation of flow fields and of shear stresses, respectively. We will examine the optimality of these rates, i. e., how the rate of convergence of the finite element approximation of smooth solutions, measured in a given norm, compares with the rate of convergence of the best approximation out of the finite element space considered. We will also be cognizant of the work and storage requirements of computer implementations of the particular finite element algorithms. Thus, having examined the rates of convergence and the computing requirements of the various algorithms, we will, at least in an asymptotic sense, be able to draw conclusions about their relative efficiency.

Finite element discretizations of our linear partial differential equations leave us with a linear system of algebraic equations to solve. A second goal of this work is to discuss the efficient implementation of

a Gauss elimination algorithm for the solution of these systems. We pay particular attention to the enforcement of the orthogonalities, both physical and nonphysical, which the discrete pressure must satisfy.

There exists an ever growing literature concerned with finite element methods for the approximate solution of both the Stokes and Navier-Stokes equations. Much of the mathematical literature is included in [1,2]. In addition, of course, there is a large body of engineering literature which is mainly directed at assessing the effectiveness of algorithms on the basis of some empirical criterion such as visual presentation of flow fields or comparison with experiments. Seldom are the asymptotic rates of convergence examined. The determination of these rates for smooth solutions of linearizations of the Navier-Stokes equations is, as described above, a goal of this work.

Section 2 contains a description of the class of problems we consider as well as a brief presentation of the analyses of error estimates. In Section 3 we introduce some particular choices of finite elements which we will use to generate the numerical results of Section 5. In Section 4, we discuss the solution of the linear systems of algebraic equations resulting from the discretization process.

2. Error Estimates

The stationary Navier-Stokes equations for the steady flow of a viscous incompressible fluid are given by

$$-\frac{1}{\mathrm{Re}}\,\mathrm{div}\,\mathrm{grad}\,\underline{u} + (\underline{u}\cdot\mathrm{grad})\underline{u} + \mathrm{grad}\,p = \underline{f} \quad \text{in} \quad \Omega \;; \tag{2.1}$$

$$\mathrm{div}\,\underline{u} = 0 \quad \text{in} \quad \Omega \;; \tag{2.2}$$

$$\underline{u} = 0 \quad \text{on} \quad \partial\Omega \;, \tag{2.3}$$

where $\underline{u}$ is the fluid velocity, p the pressure, Re the constant Reynolds number, and $\underline{f}$ a prescribed forcing function. Ω is a domain in $\mathbb{R}^2$ or $\mathbb{R}^3$ in which the velocity and pressure are sought and $\partial\Omega$ is the boundary of Ω which is assumed to be sufficiently smooth for the regularity results quoted below to hold. The variables appearing in (2.1) - (2.3) have been suitably nondimensionalized.

We wish to consider, for $\underline{x} \in \Omega$, flow fields which are "small" perturbations of a given flow field $\underline{U}(\underline{x})$. The perturbations, which we also denote by $\underline{u}$ and p, satisfy linearizations of (2.1) - (2.3) about the given flow field $\underline{U}$. Assuming that

$$\text{div } \underline{U} = 0 \quad \text{in} \quad \Omega \quad \text{and} \quad \underline{U} = 0 \quad \text{on} \quad \partial\Omega, \tag{2.4}$$

we then have the linearized Navier-Stokes equations

$$-\frac{1}{\text{Re}} \text{div grad } \underline{u} + (\underline{U} \cdot \text{grad})\underline{u} + (\underline{u} \cdot \text{grad})\underline{U} + \text{grad } p = \underline{f} \quad \text{in} \quad \Omega \; ; \tag{2.5}$$

$$\text{div } \underline{u} = 0 \quad \text{in} \quad \Omega \; ; \tag{2.6}$$

$$\underline{u} = 0 \quad \text{on} \quad \partial\Omega \; . \tag{2.7}$$

If $\underline{U} = 0$, then (2.5) - (2.7) reduce to the stationary Stokes equations while if $\underline{U}$ = constant, we are left with the Oseen equations [3].

The variational form of the problem (2.5) - (2.7) which we will employ is the following Galerkin formulation. We seek $\underline{u} \in \vec{H}_0^1(\Omega)$ and $p \in L^2(\Omega)$ such that

$$a_U(\underline{u},\underline{v}) + b(p,\underline{v}) = \langle \underline{f},\underline{v} \rangle \quad \forall \; \underline{v} \in \vec{H}_0^1(\Omega) \; ; \tag{2.8}$$

$$b(q,\underline{u}) = 0 \qquad \forall\, q \in \bar{L}^2(\Omega), \tag{2.9}$$

where

$$a_U(\underline{u},\underline{v}) = \int_\Omega \left[\frac{1}{Re}\,\mathrm{grad}\,\underline{u} : \mathrm{grad}\,\underline{v} + \underline{U}\cdot\mathrm{grad}\,\underline{u}\cdot\underline{v} + \underline{u}\cdot\mathrm{grad}\,\underline{U}\cdot\underline{v}\right] d\Omega\ , \tag{2.10}$$

$$b(q,\underline{u}) = \int_\Omega q\,\mathrm{div}\,\underline{u}\ d\Omega, \tag{2.11}$$

$$\langle \underline{f},\underline{v}\rangle = \int_\Omega \underline{f}\cdot\underline{v}\ d\Omega. \tag{2.12}$$

Here, $\vec{H}_0^1(\Omega)$ denotes the Hilbert space of real 2 or 3-dimensional vector fields whose components have distributional derivatives up to order one in $L^2(\Omega)$ in each variable and which have zero trace on $\partial\Omega$. $\bar{L}^2(\Omega)$ denotes the linear subspace of $L^2(\Omega)$ consisting of square integrable functions with zero mean over Ω. It is necessary to introduce some such normalization for the pressure since clearly (2.5) - (2.7) can determine the pressure only up to an additive constant. In (2.10) the colon denotes the scalar product of the two tensors standing on either side. We note that $\vec{H}_0^1(\Omega)$ is normed by

$$\|\underline{v}\|_1^2 = \int_\Omega \mathrm{grad}\,\underline{v} : \mathrm{grad}\,\underline{v}\ d\Omega. \tag{2.13}$$

For $\underline{f} \in \vec{H}^{-1}(\Omega)$, the dual space of $\vec{H}_0^1(\Omega)$, the form $\langle \underline{f},\underline{v}\rangle$ is a bounded linear functional on $\vec{H}_0^1(\Omega)$.

We note that for the Stokes equations, the bilinear form (2.10) reduces to

$$a_0(\underline{u},\underline{v}) = \frac{1}{Re}\int_\Omega \mathrm{grad}\,\underline{u} : \mathrm{grad}\,\underline{v}\ d\Omega,$$

which is coercive on $\vec{H}_0^1(\Omega)$ in the sense that

$$a_0(\underline{u},\underline{u}) \geq C\|\underline{u}\|_1^2 \qquad \forall\ \underline{u} \in \vec{H}_0^1(\Omega).$$

The corresponding form for the nonlinear Navier-Stokes equations is the trilinear form

$$A(\underline{w},\underline{u},\underline{v}) = a_0(\underline{u},\underline{v}) + \int_\Omega \underline{w} \cdot \operatorname{grad} \underline{u} \cdot \underline{v}\ d\Omega,$$

which is also coercive in the sense that if $\underline{w}$ is divergence free in Ω and vanishes on $\partial\Omega$, then

$$A(\underline{w},\underline{u},\underline{u}) = a_0(\underline{u},\underline{u}) \geq C\|\underline{u}\|_1^2 \qquad \forall\ \underline{w},\ \underline{u} \in \vec{H}_0^1(\Omega).$$

The bilinear form $a_U(\cdot,\cdot)$ is not coercive in this sense. In fact

$$a_U(u,u) = a_0(u,u) + \int_\Omega \underline{u} \cdot \operatorname{grad} \underline{U} \cdot \underline{u}\ d\Omega.$$

However, it can be shown by the same techniques used in [4] for non-selfadjoint second order elliptic partial differential equations that

$$\inf_{\underline{u} \in \vec{H}_0^1} \sup_{\|\underline{v}\|_1 = 1} |a_U(\underline{u},\underline{v})| \geq C\|\underline{u}\|_1, \tag{2.14}$$

and

$$\inf_{\underline{v} \in \vec{H}_0^1} \sup_{\|\underline{u}\|_1 = 1} |a_U(u,v)| \geq C\|\underline{v}\|_1. \tag{2.15}$$

Otherwise, the bilinear forms $a_U(\cdot,\cdot)$ and $b(\cdot,\cdot)$ satisfy the same continuity and stability conditions satisfied by the corresponding forms for the stationary Stokes equations. Together with (2.14) and (2.15), this enables us to apply the theory of [5] to our problem. Thus existence and uniqueness of the solution $\underline{u} \in \vec{H}_0^1(\Omega)$ and $p \in \bar{L}^2(\Omega)$ is guaranteed. Furthermore, for a sufficiently smooth boundary $\partial\Omega$ it can be shown [6] that in fact

$$\|\underline{u}\|_2 + \|p\|_1 \leq C\|\underline{f}\|_0 . \tag{2.16}$$

The finite element scheme we use is the standard one. We choose subspaces $\mathcal{V}^h \in \vec{H}_0^1(\Omega)$ and $S^h \in \bar{L}^2(\Omega)$ and then define the approximation $\underline{u}^h$ and p^h to be solutions of the problem: seek $\underline{u}^h \in \mathcal{V}^h$ and $p^h \in S^h$ such that

$$a_U(\underline{u}^h,\underline{v}^h) + b(p^h,\underline{v}^h) = \langle \underline{f},\underline{v}^h \rangle \quad \forall \ \underline{v}^h \in \mathcal{V}^h, \tag{2.17}$$

$$b(q^h,\underline{u}^h) = 0 \qquad \forall \ q^h \in S^h. \tag{2.18}$$

The existence and uniqueness of the approximations $\underline{u}^h$ and p^h follow when the forms $a_U(\cdot,\cdot)$ and $b(\cdot,\cdot)$ satify certain continuity and stability conditions on the discrete spaces. Since this analysis closely parallels that for the stationary Stokes equations [7], we omit it here.

The analysis of the error between the solution of (2.8), (2.9) and (2.17), (2.18) is also given in [7] with generalizations given in [5]. These analyses are based on the application of the Babuška theory to the variational problem: seek $(\underline{u},p) \in \vec{H}_0^1 \times \bar{L}^2$ such that

$$B[(\underline{u},p),(\underline{v},q)] = <\underline{f},\underline{v}> \quad \forall\ (\underline{v},q) \in \vec{H}_0^1 \times \bar{L}^2,$$

where

$$B[(\underline{u},p),(\underline{v},q)] \equiv a_U(\underline{u},\underline{v}) + b(p,\underline{v}) + b(q,\underline{u}).$$

This variational formulation over the product space $\vec{H}_0^1 \times \bar{L}^2$ is obtained from the formulation (2.8), (2.9) in the obvious manner. The resulting error estimate is obtained in the graph norm

$$|||(\underline{v},q)||| \equiv \|\underline{v}\|_1 + \|q\|_0,$$

and is given by

$$|||(\underline{u}-\underline{u}^h,p-p^h)||| \leq C \inf |||(\underline{u}-\hat{\underline{u}}^h,p-\hat{p}^h)|||, \tag{2.19}$$

where the infimum is taken over all $(\hat{u}^h,\hat{p}^h) \in V^h \times S^h$. The estimate (2.19) immediately yields that

$$\|\underline{u}-\underline{u}^h\|_1 \leq C\left\{ \inf_{\hat{\underline{u}}^h \in V^h} \|\underline{u}-\hat{\underline{u}}^h\|_1 + \inf_{\hat{p}^h \in S^h} \|p-\hat{p}^h\|_0 \right\}, \tag{2.20}$$

with a similar estimate for $\|p-p^h\|_0$.

More precise estimates can be deduced as a direct application of the theory given in [8]. Before presenting these estimates, we need to introduce the subspaces $Z \subset \vec{H}_0^1(\Omega)$ and $Z^h \subset V^h$ defined by

$$Z = \{\underline{z} \in \vec{H}_0^1(\Omega) \,\big|\, b(q,\underline{z}) = 0 \quad \forall\ q \in \bar{L}^2(\Omega)\},$$

and

$$Z^h = \{\underline{z}^h \in V^h \mid b(q^h, \underline{z}^h) = 0 \ \forall \ q^h \in S^h\}.$$

Roughly speaking, Z is the subspace of $\vec{H}_0^1(\Omega)$ consisting of solenoidal fields and Z^h is the subspace of V^h consisting of "discretely solenoidal" fields. It is important to note that in general, $Z^h \not\subset Z$. We also define

$$\Gamma(Z,Z^h) \equiv \sup \inf \| \underline{z} - \underline{z}^h \|_1 \ ,$$

where the infimum is taken over all $\underline{z} \in Z$ and the supremum is taken over all $\underline{z}^h \in Z^h$ with $\| \underline{z}^h \|_1 = 1$. If $Z^h \subset Z$ then clearly $\Gamma(Z,Z^h) = 0$. In general, $\Gamma(Z,Z^h)$ is a measure of the angle between the linear manifolds Z and Z^h and clearly, from its definition, $0 \leq \Gamma(Z,Z^h) \leq 1$. Then, applying the analysis of [8], we are led to the error estimates

$$\| \underline{u} - \underline{u}^h \|_1 \leq C_1 \inf_{\hat{\underline{u}}^h \in V^h} \| \underline{u} - \hat{\underline{u}}^h \|_1 + C_2 \Gamma(Z,Z^h) \inf_{\hat{p}^h \in S^h} \| p - \hat{p}^h \|_0 , \qquad (2.21)$$

and

$$\| p - p^h \|_0 \leq C_1' \inf_{\hat{\underline{u}}^h \in V^h} \| \underline{u} - \hat{\underline{u}}^h \|_1 + C_2' \inf_{\hat{p}^h \in S^h} \| p - \hat{p}^h \|_0 . \qquad (2.22)$$

The estimate (2.22) is essentially the same as the corresponding estimate obtained from the graph norm estimate (2.19). The estimate (2.21), when compared to (2.20) contains new information in the mulitplier $\Gamma(Z,Z^h)$. For example, if $Z^h \subset Z$, then (2.21) reduces to

$$\| \underline{u} - \underline{u}^h \|_1 \leq C \inf_{\hat{\underline{u}}^h \in V^h} \| \underline{u} - \hat{\underline{u}}^h \|_1 , \qquad (2.23)$$

i. e., the error in the velocity field uncouples from that of the pressure field. We believe, although it has not been proven, that the estimates (2.21), (2.22) are sharp, even when $\Gamma(Z,Z^h) \neq 0$. For these reasons we will regard (2.21), (2.22) to be our estimate for the velocity error in the $\vec{H}_0^1(\Omega)$ norm and the pressure error in the $\vec{L}^2(\Omega)$ norm.

Provided $\underline{u}$ is sufficiently smooth, the standard duality argument may be applied to obtain an estimate for the velocity error in the $\vec{L}^2(\Omega)$ norm

$$\|\underline{v}\|_0 = \int_\Omega \left[\underline{v} \cdot \underline{v} \right]^{\frac{1}{2}} d\Omega.$$

The result is, as expected [2], that

$$\|\underline{u}-\underline{u}^h\|_0 \leq C\left\{\|\underline{u}-\underline{u}^h\|_1 + \|p-p^h\|_0\right\} \sup_{\underline{g} \in \vec{L}^2} \left[\frac{1}{\|\underline{g}\|_0}\left\{\inf_{\underline{v}^h \in V^h} \|\underline{v}_g - \underline{v}^h\|_1 + \inf_{q^h \in S^h} \|q_g - q^h\|_0\right\}\right] . \tag{2.24}$$

where $(\underline{v}_g, q_g)$ is the solution of the adjoint problem

$$a_U^*(\underline{u},\underline{v}_g) + b(\underline{u},q_g) = \langle \underline{g},\underline{u}\rangle \quad \forall\ \underline{u} \in \vec{H}_0^1(\Omega) , \tag{2.25}$$

$$b(\underline{v}_g,p) = 0 \qquad \forall\ p \in \bar{L}^2(\Omega) , \tag{2.26}$$

and where

$$a_U^*(\underline{u},\underline{v}) = a_0(\underline{u},\underline{v}) + \int_\Omega [\underline{u} \cdot \text{grad } \underline{U} \cdot \underline{v} - U \cdot \text{grad } \underline{v} \cdot \underline{u}]\, d\Omega.$$

The existence and uniqueness of the solutions of the adjoint problem (2.25), (2.26) follows from the conditions on the forms $a_U(\cdot,\cdot)$ and $b(\cdot,\cdot)$ which guarantee the existence and uniqueness of the solution of the problem (2.8), (2.9). Furthermore, for $\partial\Omega$ smooth enough, the solution $(\underline{v}_g, q_g)$ also satisfies a regularity estimate of the type (2.13), i.e., we have that

$$\|\underline{v}_g\|_2 + \|q_g\|_1 \leq c\|\underline{g}\|_0 .$$

3. Finite Element Pairs

The problem (2.8), (2.9) is not positive definite and therefore discrete approximation procedures tend to be unstable. Therefore, some care must be exercised in the choice of the approximating spaces V^h and S^h. There are several conditions that must hold for the stability of the approximations to be guaranteed; these may be found, e.g. in [5] or [8]. The particular form of these conditions which we will use is now introduced. Let W^h denote the orthogonal complement of Z^h in V^h with respect to the inner product

$$\int_\Omega \nabla \underline{u} : \nabla \underline{v} \, d\Omega .$$

Then

$$V^h = Z^h \oplus W^h. \tag{3.1}$$

Further, let the operator $\mathrm{div}_h : V^h \to S^h$ be defined by the relation

$$b(q^h, \underline{v}^h) \equiv \int_\Omega q^h \, \mathrm{div}_h \underline{v}^h \qquad \forall\ q^h \in S^h, \tag{3.2}$$

where $b(\cdot,\cdot)$ is defined by (2.11). The conditions necessary for the existence of the decomposition (3.1) and the operator div_h will always hold for the problem set up in the form (2.17), (2.18). Details can be found in, e.g. [5] and [8]. The necessary stability condition is the following: there exists a positive constant γ independent of h (which for our purposes is a measure of the grid size) such that

$$\| \mathrm{div}_h \underline{w}^h \|_0 \geq \gamma \| \underline{w}^h \|_1 \qquad \forall\ \underline{w}^h \in W^h. \tag{3.3}$$

For given subspaces S^h and V^h, it is not in general easy to prove that (3.3) holds. Clearly, since the form $b(\cdot,\cdot)$ is identical to the corresponding form for the stationary Stokes equations, the stability criterion (3.3) is the same as that necessary for that simpler case. For the element pairs considered below, the condition (3.3) has been shown to hold [9].

It is easy to show that (3.3) does not hold in general. To see this, take Ω to be a square. We subdivide the square into subsquares and then into triangles as shown in Figure 1. We choose V^h to be the space of vector valued functions with components which are continuous piecewise linear polynomials defined on the triangles which also vanish on the boundary $\partial\Omega$. For S^h, we choose all piecewise constant functions on the triangles with zero mean over the square. From (3.2) it is simple to show that

$$\mathrm{div}_h\, \underline{v}^h = \mathrm{div}\, \underline{v}^h \qquad \forall\ \underline{v}^h \in V^h.$$

On the other hand, by inspection of Figure 1 and the use of the boundary condition $\underline{v}^h = 0$ on $\partial\Omega$ shows that $\mathrm{div}\, \underline{v}^h = 0$ implies that $\underline{v}^h = 0$. But then $Z^h = 0$ so that $W^h = V^h$ and therefore (3.3) must hold for all

$\underline{v}^h \in V^h$. But clearly we may choose $\underline{v}^h$ such that $\| \underline{v}^h \|_1 = 1$ and $\underline{v}^h$ is a best $\vec{H}_0^1(\Omega)$ approximation to a solenoidal field. Then

$$\| \operatorname{div}_h \underline{v}^h \|_0 \to 0 \quad \text{as} \quad h \to 0,$$

so that (3.3) cannot hold.

In choosing V^h and S^h, a triangulation of Ω must be established for V^h and another one for S^h. There is no a priori reason for these two triangulations to be coincident, although in the literature this is often the case. Some of the element discussed below use different, although related, trianglulations for V^h and S^h.

Once triangulations for V^h and S^h are chosen, some discussion must be made about the degrees of the element polynomials in each case. The estimate (2.21) indicates that if the mesh sizes of V^h and S^h are comparable, then since $0 \leq \Gamma(Z,Z^h) \leq 1$, it is desirable to choose the degrees of the element polynomials so that the two terms on the right hand side of (2.21) are of the same order in h. We refer to this condition on the degrees of the element polynomials as the "comparability condition" between the spaces V^h and S^h. We shall see below that this condition is not necessary for the $\vec{H}_0^1(\Omega)$ convergence of the velocity approximations. On the other hand, some of computational results of section 5 indicate that the comparability condition is probably necessary for optimal $\vec{H}_0^1(\Omega)$ convergence. It is assumed, of course, that the chosen elements form a stable combination in the sense of (3.3).

Below we describe four finite element pairs. In each case we define a space V^h of discrete velocities and a space $\tilde{S}^h$ of discrete pressures. The spaces $\tilde{S}^h$ so defined are not subspaces of $\bar{L}^2(\Omega)$ and must therefore be constrained to satisfy the zero mean condition. In some instances, the

spaces $\tilde{S}^h$ must be further contrained in order for the stability condition (3.3) to be satisfied. In $\mathbb{R}^2$ this additional constraint takes the form of a single orthogonality condition which the discrete pressure must satisfy. The subspace of $\tilde{S}^h$ obtained by imposing the above constraints on the space $\tilde{S}^h$ of discrete pressures. Details about the nature and implementation of such constraints are given below in section 4.

A stable scheme, apparently first suggested in [7] is obtained by subdividing Ω into triangles and then choosing $\tilde{S}^h$ to be all piecewise constant functions over the triangles and V^h to be all continuous piecewise quadratic vector fields over the triangles which vanish on the boundary $\partial\Omega$. The approximations found using these subspaces are optimal in the graph norm estimate (2.19) [2] but, as the computations reported below indicate, the approximation to the velocity field is not optimal in the $\vec{H}_0^1(\Omega)$ norm. We note that the comparability condition is not satisfied by this quadratic constant element pair. Furthermore, it is clear that $\text{div}_h \neq \text{div}$, i.e., $Z^h \not\subset Z$, since the divergence of elements in V^h will in general be piecewise linear functions while $\text{div}_h \underline{v}^h$, being by definition an element of S^h, is a piecewise constant function.

A second stable scheme is defined as follows. First, subdivide Ω into quadrilaterals and choose $\tilde{S}^h$ to be all piecewise constant functions over the quadrilaterals. We then subdivide each quadrilateral into triangles by drawing a diagonal and choose V^h to be all continuous piecewise linear vector fields over the triangles which vanish on the boundary $\partial\Omega$. Here we are using distinct, although closely related, triangulations in defining V^h and $\tilde{S}^h$. Furthermore, once again it is clear that $\text{div}_h \neq \text{div}$, i.e., $Z^h \not\subset Z$. On the other hand, the comparability condition is satisfied. Computational results displaying optimal $\vec{H}_0^1(\Omega)$ accuracy in the velocity approximations are reported below.

The third scheme we study has the distinguishing feature that $\text{div}_h = \text{div}\ v$ so that $Z^h \subset Z$ and $\Gamma(Z,Z^h) = 0$. Also this scheme is stable and satisfies the comparability condition. To define this scheme, we again subdivide Ω into quadrilaterals and subsequently divide each quadrilateral into four triangles by drawing both diagonals. Then V^h is chosen to be all continuous linear vector fields over the triangles which vanish on the boundary $\partial\Omega$ and $\tilde{S}^h$ is chosen to be $\tilde{S}^h \equiv \text{div}\ V^h$. $\tilde{S}^h$ is a subspace of the space of all piecewise constant functions defined over the triangles. Referring to Figure 2, a convenient basis for $\tilde{S}^h$ is defined within a quadrilateral ABCD by the three functions which are constants on the triangles ABD, ABC and BCD and zero elsewhere. The basis set is three dimensional within each quadrilateral, instead of being four dimensional, because the divergence theorem forces a constraint within each quadrilateral. It can be shown that $\tilde{S}^h$ possesses essentially the same approximation property as that for the space of all piecewise constant functions over the triangles. More details concerning this element pair may be found in [10].

The fourth and final scheme, unlike the three previous ones, is restricted to regions whose boundaries are straight lines parallel to the coordinate axes. We subdivide such a region into rectangles and choose $\tilde{S}^h$ to be all piecewise constant functions over the rectangles and V^h to be all continuous piecewise bilinear vector fields over the rectangles which vanish on the boundary $\partial\Omega$. Clearly, for this element pair, $\text{div}_h \neq \text{div}$ but the comparability condition holds and we can expect optimal $\vec{H}_0^1(\Omega)$ accuracy for the velocity approximations.

4. Direct Solution of Discrete Equations

The discrete linear system of equations resulting from using the above finite element pairs V^h, $\tilde{S}^h$ in (2.17), (2.18) is indefinite, and due to the convection terms depending on $\underline{U}$, is non-symmetric. If the unknowns are numbered sequentially according to nodes, the coefficient matrix is also banded. Due to the indefiniteness of the system, a partial pivoting strategy must be used.

For all the element pairs introduced in section 3, the computed pressure should be normalized so that it has zero mean. Except for the quadratic-constant element pair, there may be an additional orthogonality condition which the discrete pressure must satisfy. To see how the need for such a condition arises, let us consider the second element pair introduced in section 3. It is easy to verify that for a rectangular uniform grid, the discrete pressure gradient at the point P (see Figure 3) is given by the vector

$$\begin{pmatrix} [(p_2+p_4)-(p_1+p_3)]/2\Delta x \\ [(p_1+p_2)-(p_3+p_4)]/2\Delta y \end{pmatrix} . \tag{4.1}$$

where p_i refers to the constant discrete pressure in the box labled i. Clearly this discrete gradient vanishes not only for the constant function $p_1 = p_2 = p_3 = p_4$ but also for the piecewise constant function $p_1 = -p_2 = -p_3 = p_4$. The latter function is in the null space of the discrete gradient due to the averaging process which precedes the differencing process in (4.1). In triangulations which can be obtained from a regular triangulation by piecewise linear mappings the quadrilaterals which subdivide Ω can be labeled red and black in a checkerboard pattern. Then the discrete gradient operator will have a two dimensional null space consisting of the

constant function and a function analogous to the osciallating function described above for the grid of Figure 3. Indeed, if Ω is a rectangle and the triangulation is uniform, this function is equal to one on the black boxes and minus one on the red boxes. This phenomena also occurs for the third and fourth element pairs of section 3. It is important to note that in general it is not necessary to know a priori the number of elements in the null space of the gradient or their exact nature. The correct normalization of the discrete pressure may be accomplished without such information, e.g. by the process described in the next three paragraphs.

It was found convenient not to impose any normalization or orthogonality conditions on the approximating space $\tilde{S}^h$ for the pressure but instead to impose these conditions on the discrete pressure by a post-processing procedure. Then, during the elimination process, zero pivot elements are encountered. The number of such elements is equal to the dimension of the null space of the discrete gradient operator, i.e. one for the quadratic-constant element pair and perhaps two for the other three element pairs. In the actual computations, these pivot elements are detected whenever a pivot is encountered whose magnitude is smaller than a prescribed tolerance which should depend on the machine precision. When a zero pivot is encountered, that step of the elimination process may be skipped since the corresponding column to be eliminated is already in reduced form. Then, during the backsolve, the components of the solution vector corresponding to the zero pivots may be arbitrarily prescribed, i.e., they may be set to unity.

Of course, the discrete pressure found by this process will not satisfy any of the normalization or orthogonality conditions. However, these may now be imposed on the solution of the discrete equations by a simple

post-processing procedure which renders the discrete pressure orthogonal to the null space of the discrete gradient. We note that the discrete velocity field computed by the elimination procedure described above is correct and thus needs no further processing. To describe the post-processing procedure for the discrete pressure, let us denote by $\vec{P}'$ the vector whose components P'_j are the discrete pressure in the j-th pressure element (triangles for the quadratic-constant element pair, quadrilaterals for the second element introduced in section 3, etc). Then $\vec{P}'$ is an element of $\mathbb{R}^J$ where J is the number of pressure elements. Now let $\{\vec{S}^h\}$, $k = 1,\ldots,K$ denote an orthogonal basis for the null space of the discrete gradient operator, where $K = 1$ for the quadratic-constant element pair and K may be 2 for the other three element pairs. (Incidentally, the discrete gradient operator, being a linear operator between the finite dimensional spaces $\tilde{S}^h$ and V^h, may be expressed as a matrix. Indeed, the discrete divergence operator div_h has the matrix representation D whose elements are given by

$$D_{mn} = b(q_m, \underline{v}_n),$$

where $\{q_m\}$ and $\{\underline{v}_n\}$ are basis sets for S^h and V^h, respectively. Then the discrete gradient operator may be represented by D^T.) We then define $\vec{P} \in \mathbb{R}^J$ by

$$\vec{P} = \left(I - \sum_{k=1}^{K} \frac{\vec{S}^k (\vec{S}^k)^T}{(\vec{S}^k)^T \vec{S}^k} \right) \vec{P}' .$$

Then the piecewise constant function p^h whose value in the j-th pressure element is given by the j-th component of $\vec{P}$, i.e. P_j, is the post-processed

discrete pressure which we seek, i.e. p^h will satisfy all the required orthogonality and normalization conditions.

For some simple geometries and triangulations, it is possible to determine the vectors $\{\vec{S}^k\}$ by inspection. In the general case, they may be determined, with negligible additional cost, as follows. When we perform the backsolve step in the elimination procedure, we do it with either one or two additional right hand sides, depending on the particular element pair being used. These additional right hand sides have all components equal to zero. When the first zero pivot element is reached during the backsolve, the corresponding element in the solution vector corresponding to the first additional right hand side is set equal to unity, while for the second right hand side, if it is necessary, it is set equal to zero. If a second zero pivot element is reached, the above assignments of the corresponding components in the solution vectors are reversed. At the end of the elimination procedure, the solution vectors corresponding to the additional right hand sides will contain, in their components which are discrete pressures, a basis for the null space of the discrete gradient operator. The $\{\vec{S}^k\}$ found this way will in general not be orthogonal; of course and orthogonal basis is found, again at negligible cost, by replacing $\vec{S}^2$ by

$$\left(I - \frac{\vec{S}^1(\vec{S}^1)^T}{(\vec{S}^1)^T\vec{S}^1}\right)\vec{S}^2 \quad .$$

The storage and computing time required by the four schemes described in section 3 differ sharply. As an example, let Ω be a rectangle subdivided into an $N \times N$ grid, i. e. N boxes in both the x and y direction. Then the grid size h is proportional to $1/N$. In Table 1

we tabulate the number of unknowns and half-bandwidth of the coefficient matrices resulting from each scheme. The tabulated expressions are valid for large N, i.e. we only give the leading term in N. We also give the storage and computing time requirements for each element pair relative to those for the quadratic-constant element pair.

TABLE 1

Storage and Computing Time Requirements

Element Pair	Number of Unknowns	Half-bandwidth	Relative Storage	Relative Computing Time
QC	$10N^2$	10N	1	1
LC2	$3N^2$	3N	.09	.027
LC4	$7N^2$	7N	.49	.343
BC	$3N^2$	3N	.09	.027

In the table, QC refers to the quadratic constant element pair, LC2 and LC4 to the linear-constant element pairs with two and four triangles per quadrilateral, respectively, and BC to the bilinear-constant element pair. Clearly the element pairs LC2 and BC require significantly less storage and computing time. This is significant since, as we shall see in the next section, all four element pairs achieve the same rates of convergence.

5. Computational Results

In order to compute the asymptotic error behavior as a function of the grid size h, (2.5) - (2.7) was solved in the region

$$\Omega = \{x,y \mid 0 < x,y < 1\},$$

for a problem whose exact solution is

$$\underline{u} = \begin{pmatrix} \sin \pi x \sin 2\pi y \\ x^2(1-x)\sin \pi y \end{pmatrix}$$

$$p = (1 - 4y + y^3)\cos \pi x.$$

For this choice of $\underline{u}$ and p (2.7) is satisfied, but (2.6) is actually inhomogeneous, i.e. (2.6) is replaced by $\operatorname{div} \underline{u} = F$ where F is a smooth function $\neq 0$. Generally in incompressible flows $F = 0$ but the fact that here it is nonzero does not affect the validity of the results below when $F = 0$. This is because for smooth solutions the rates of convergence in the estimates (2.21), (2.22) and (2.24) are independent of $\underline{f}$ and F. For instance, in (2.21), using linear velocity and constant pressure elements we obtain

$$\| \underline{u} - \underline{u}^h \|_1 \leq Ch(\| \underline{u} \|_2 + \| p \|_1),$$

and only the multiplier of h depends on $\underline{f}$ and F. Indeed, for $F \neq 0$, the regularity estimate (2.16) is replaced by

$$\| \underline{u} \|_2 + \| p \|_1 \leq C(\| \underline{f} \|_0 + \| F \|_1).$$

We will use the notation of Table 1 in labeling the element pairs. In all cases the triangulation of Ω used was a uniform one based on subdividing Ω into smaller squares of side h and, when called for, further subdividing these squares into triangles. Although the problems and regions considered here are rather simple, they suffice to determine the asymptotic rates of convergence of the approximations.

Two different choices for the convection velocity U were employed, namely

$$U = \begin{pmatrix} \frac{1}{2} \\ \\ \frac{1}{2} \end{pmatrix} \qquad \text{and} \qquad U = \begin{pmatrix} 4(y - y^2) \\ \\ 0 \end{pmatrix} .$$

For the first choice the problem (2.5) - (2.7) describes an Oseen flow while for the second choice we have a linearization about a parallel flow with a parabolic velocity profile.

Instead of computing the error $\underline{u} - \underline{u}^h$, we actually computed $\underline{u}^h - \tilde{\underline{u}}^h$, where $\tilde{\underline{u}}^h = I_h \underline{u}$ and I_h is the pointwise interpolation operator from $\underline{u} \to \tilde{\underline{u}}^h \in V^h$. Then the norms

$$\| \tilde{\underline{u}}^h - \underline{u}^h \|_1 \qquad \text{and} \qquad \| \tilde{\underline{u}}^h - \underline{u}^h \|_0 \quad , \tag{5.1}$$

were computed. The reason for comparing with the interpolate is that the norms (5.1) may be easily computed exactly (except, of course, for roundoff errors). Then, by the triangle inequality,

$$\| \underline{u} - \underline{u}^h \|_* \leq \| \underline{u} - \tilde{\underline{u}}^h \|_* + \| \tilde{\underline{u}}^h - \underline{u}^h \|_* \quad , \tag{5.2}$$

where $\| \cdot \|_*$ denotes either of the norms in (5.1). The first term on the right of (5.2) is purely approximation theoretical and can be easily estimated for smooth solutions. The second term on the right will be estimated by the computations reported below.

The errors in the pressure were also computed relative to an interpolant. For the element pair QC this interpolant was the S^h - interpolant with the interpolation points being the centroids of the triangles.

For LC2 and BC element pairs the S^h - interpolant was again used with the interpolation points being the centroids of quadrilaterals. For the LC4 grid, we used the interpolant on the space of all piecewise constant functions over the quadrilaterals, with the interpolation points being the centroids of quadrilaterals. Furthermore, for the LC4 grid we replace p^h by the average value of p^h over each quadrilateral.

The rates of convergence were calculated by assuming that the errors in every case have the form Ch^α and then computing α between each pair of successive grids by the formula

$$\alpha = \ell n\left(\frac{\varepsilon_2}{\varepsilon_1}\right) \Big/ \ell n\left(\frac{h_2}{h_1}\right) ,$$

where ε_i denotes any of the errors.

Tables 2-5 contain the computed convergence rates for the $\vec{L}^2(\Omega)$ error in the pressure approximation and the $\vec{L}^2(\Omega)$ and $\vec{H}_0^1(\Omega)$ errors in the velocity approximation for each of the four element pairs. A sequence of grids ranging from $h = 1/7$ to $h = 1/14$ were used to generate the entries in the table.

For the element pairs LC2, LC4 and BC, the rates given in the tables are at least as great as the correponding rates for the approximation error. Therefore, by (5.2) the rate of convergence will be no worse than that given by the approximation theoretic part, i.e., convergence is optimal. In these three cases,

$$\begin{aligned} \| p - p^h \|_0 &= O(h) \\ \| \underline{u} - \underline{u}^h \|_1 &= O(h) \\ \| \underline{u} - \underline{u}^h \|_0 &= O(h^2). \end{aligned} \tag{5.3}$$

On the other hand, the rates given in Table 2 show that in (5.2) the velocity errrors are dominated by the second term on the right hand side. The $\vec{H}_0^1$ and $\vec{L}^2$ approximation errors are $O(h^2)$ and $O(h^3)$, respectively, while by Table 2 the corresponding second terms in (5.2) are $O(h)$ and $O(h^2)$, respectively. Strictly speaking this does not imply that $\| \underline{u} - \underline{u}^h \|_1$ is not $O(h^2)$ and $\| \underline{u} - \underline{u}^h \|_0 \neq O(h^3)$; however, direct computation of these errors, based on the use of high order quadrature formulas, show that these errors are indeed at best $O(h)$ and $O(h^2)$, respectively, i.e. the rates are sub-optimal. In fact, the estimates (5.3) hold for the element pair QC, in spite of the fact that it is considerably more complex to compute with than the other element pairs (see Table 1).

If we allow the Reynolds number to become very small, then (2.5) begins to look more and more like a Poisson equation for the components of $\underline{u}$. Not surprisingly, this improves the rates of convergence of the velocity approximation for the element pair QC relative to the rates given in Table 2, i.e. they approach the optimal rates. Of course, the rate for the other element pairs are unaffected since they were already optimal.

We note that in some instances the rates measured relative to the interpolant are one order higher than the corresponding rates for the approximation error. This happens for all the pressure errors and for the $\vec{H}_0^1$ velocity errors for the element pairs LC2 and BC. This form of "superconvergence" is potentially useful, for example when linear functionals of the true solution are to be approximated.

Finally we note that the estimates given in (5.3) are everywhere in agreement with corresponding theoretical estimates (2.21), (2.22) and (2.24). Therefore, it seems that the latter are indeed sharp.

References

[1] Teman, R., Navier-Stokes Equations, North-Holland, Amsterdam (1979).

[2] Girault, V. and P.-A. Raviart, Finite Element Approximations of the Navier-Stokes Equations, Lecture Notes in Mathematics, 749, Springer-Verlag, Berlin (1979).

[3] Schlichting, H., Boundary Layer Theory, Mc-Graw-Hill, New York (1960).

[4] Babuška, I. and A. K. Aziz, "Survey lectures on the mathematical foundations of the finite element method," in The Mathematical Aspects of the Finite Element Method with Applications to Partial Differential Equations, ed. A. K. Aziz, Academic Press, (1972), pp. 1-359.

[5] Brezzi, F., "On the existence, uniqueness and approximation of saddle point problems arising from Lagrange multipliers," RAIRO, 8-R2, (1974), pp. 129-151.

[6] Agmon, S., A. Douglis, and L. Nirenberg, "Estimates near the boundary for solutions of elliptic partial differential equations satisfying general boundary conditions II," Comm. Pure Appl. Math., 17, (1964), pp. 35-92.

[7] Crouzeix, M. and P.-A. Raviart, "Conforming and non-conforming finite element methods for solving the stationary Stokes equations," RAIRO, 7-R2, (1973), pp. 33-76.

[8] Nicolaides, R. A., "Existence, uniqueness and approximation for generalized saddle point problems," ICASE Report No. 79-22, to appear in SIAM J. on Numer. Anal.

[9] Fix, G. J., "A general theory for mixed finite element methods," to appear.

[10] Fix, G. J., M. D. Gunzburger, and R. A. Nicolaides, "On mixed finite element methods for first order elliptic systems," ICASE Report No. 81-3, to appear in Numer. Math.

TABLE 2

Rates of Convergence for the Element Pair QC

h	Oseen Flow			Parallel Flow		
	p in L_2	$\underline{u}$ in $\vec{H}^1$	$\underline{u}$ in $\vec{L}^2$	p in L_2	$\underline{u}$ in $\vec{H}^1$	$\underline{u}$ in $\vec{L}^2$
1/7	1.645	1.028	1.904	1.643	1.028	1.905
1/8	1.662	1.002	1.902	1.660	1.001	1.903
1/9	1.678	.986	1.904	1.676	.986	1.905
1/10	1.692	.977	1.908	1.690	.977	1.908
1/11	1.704	.973	1.912	1.703	.972	1.912
1/12	1.716	.970	1.916	1.714	.970	1.916
1/13	1.724	.969	1.920	1.724	.968	1.920
1/14						

TABLE 3

Rates of Convergence for the Element Pair LC2

h	Oseen Flow			Parallel Flow		
	p in L_2	$\underline{u}$ in $\vec{H}^1$	$\underline{u}$ in $\vec{L}^2$	p in L_2	$\underline{u}$ in $\vec{H}^1$	$\underline{u}$ in $\vec{L}^2$
1/7	2.513	2.083	2.021	2.152	2.084	2.022
1/8	2.248	2.064	2.014	2.249	2.065	2.015
1/9	2.100	2.052	2.007	2.108	2.063	2.024
1/10	2.147	2.037	2.005	2.137	2.026	1.988
1/11	2.019	2.022	2.002	2.039	2.032	2.004
1/12	2.152	2.034	2.003	2.130	2.030	2.002
1/13	2.007	2.023	2.001	2.023	2.030	2.011
1/14						

TABLE 4

Rates of Convergence for the Element Pair LC4

h	Oseen Flow			Parallel Flow		
	p in L^2	$\underline{u}$ in $\vec{H}^1$	$\underline{u}$ in $\vec{L}^2$	p in L^2	$\underline{u}$ in $\vec{H}^1$	$\underline{u}$ in $\vec{L}^2$
1/7						
	2.182	1.028	2.157	2.244	1.027	2.101
1/8						
	2.185	1.019	2.082	2.301	1.020	2.045
1/9						
	2.057	1.015	2.091	2.160	1.014	2.008
1/10						
	2.132	1.010	2.061	2.302	1.011	1.978
1/11						
	1.982	1.008	2.062	2.161	1.007	1.947
1/12						
	2.099	1.008	2.042	2.298	1.008	1.891
1/13						
	1.915	1.006	2.042	2.127	1.006	1.857
1/14						

TABLE 5

Rates of Convergence for the Element Pair BC

h	Oseen Flow			Parallel Flow		
	p in L^2	$\underline{u}$ in $\vec{H}^1$	$\underline{u}$ in $\vec{L}^2$	p in L^2	$\underline{u}$ in $\vec{H}^1$	$\underline{u}$ in $\vec{L}^2$
1/7						
	2.100	2.038	1.988	2.286	2.091	2.051
1/8						
	2.309	2.026	1.989	2.458	2.027	1.998
1/9						
	1.970	2.017	1.988	2.220	2.083	2.065
1/10						
	2.289	2.017	1.993	2.570	2.034	2.023
1/11						
	1.930	2.026	2.006	2.167	2.068	2.066
1/12						
	2.249	1.995	1.978	2.780	2.057	2.062
1/13						
	1.821	2.007	1.992	2.121	2.057	2.072
1/14						

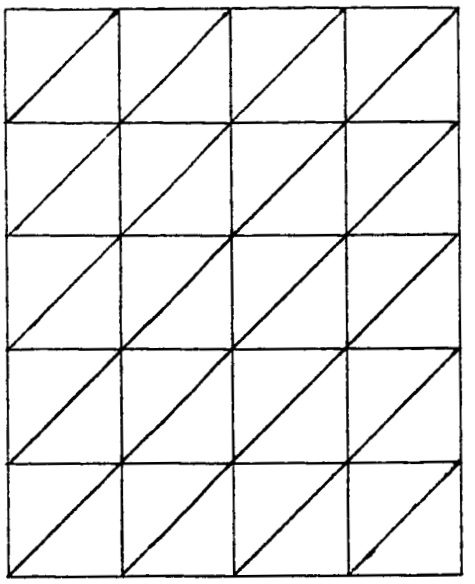

Figure 1. A grid not satisfying the stability criterion (3.3).

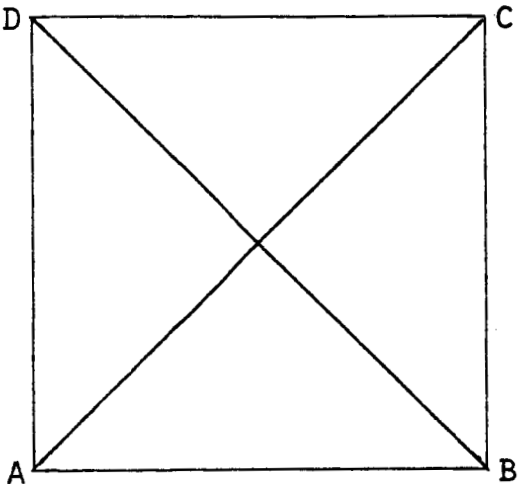

Figure 2. Triangulation of a quadrilateral for the LC4 element pair.

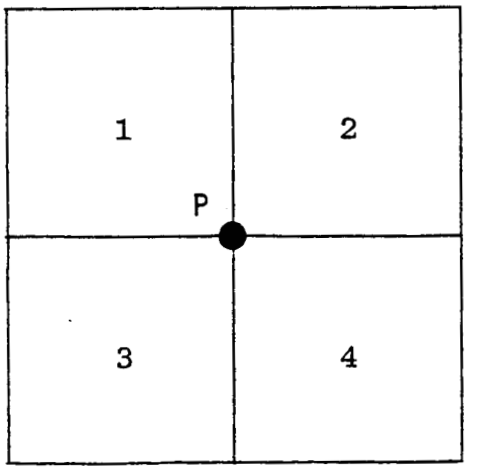

Figure 3. Discrete pressure elements for the LC2 element pair.